Development and characterization of chitosan films carrying Artemisia campestris antioxidants for potential use as active food packaging materials

Salma Moalla, Imène Ammar, Marie Laure Fauconnier, Sabine Danthine, Christophe Blecker, Souhail Besbes, Hamadi Attia

PII: S0141-8130(21)00879-5

DOI: https://doi.org/10.1016/j.ijbiomac.2021.04.113

Reference: BIOMAC 18364

To appear in: *International Journal of Biological Macromolecules*

Received date: 30 December 2020

Revised date: 10 April 2021

Accepted date: 17 April 2021

Please cite this article as: S. Moalla, I. Ammar, M.L. Fauconnier, et al., Development and characterization of chitosan films carrying Artemisia campestris antioxidants for potential use as active food packaging materials, *International Journal of Biological Macromolecules* (2018), https://doi.org/10.1016/j.ijbiomac.2021.04.113

Development and characterization of chitosan films carrying *Artemisia campestris* antioxidants for potential use as active food packaging materials

Salma MOALLA[a*], Imène AMMAR[a], Marie‐Laure FAUCONNIER[b], Sabine DANTHINE[c], Christophe BLECKER[c], Souhail BESBES[a], Hamadi ATTIA[a]

[a] Laboratory of Analysis, Valorization and Food Safety, Department of Biology, National School of Engineers of Sfax, University of Sfax, Soukra Road, 3038 Sfax, Tunisia.

[b] General and Organic Chemistry‐Volatolomics, Gembloux Agro‐Bio Tech, University of Liège, Passage des Déportés 2, 5030 Gembloux, Belgium.

[c] Laboratory of Food Science and Formulation, Faculty of Gembloux Agro-Bio Tech, University of Liège, Avenue de la faculté 2-B, 5030 Gembloux, Belgium.

[*] Corresponding author. Tel. +21655056743, Soukra Road, 3038 Sfax, Tunisia.
E-mail adress: salma.moallaa@gmail.com

Abstract

Active food packaging films based on chitosan and enriched with *Artemisia campestris* hydroalcoholic extract (ACHE), aqueous extract (ACAE) and essential oil (ACEO) were developed. The effects of incorporating *A. campestris* were investigated on the physical, mechanical, thermal and antioxidant characteristics of the films. The structural properties of the films were evaluated using Fourier transform infrared (FTIR) spectroscopy, X-ray diffraction (XRD) and scanning electron microscopy (SEM). The results showed that adding ACHE and ACEO improved the water resistance of chitosan films. The FTIR spectroscopy analysis revealed covalent interaction and hydrogen bonding between chitosan and ACHE. The XRD and SEM analyses indicated that interactions occurred between the film matrix and *A. campestris* active compounds, which could be reflected by the physical and mechanical properties of composite films. Incorporating ACHE and ACAE in the chitosan matrix decreased the tensile strength. The film extensibility was reduced when ACHE and ACEO were added. All films exhibited great thermal stability as the degradation occurred above 300 °C. The addition of *A. campestris* active compounds, particularly extracts, to chitosan films notably increased the antioxidant and UV-Vis barrier properties. Chitosan films enriched with the *A. campestris* antioxidant compounds could be applied as food packaging alternatives.

Keywords: *Artemisia campestris*; Active film; Chitosan; Antioxidant; Polyphenols; Essential oil.

1. Introduction

The food packaging process is of paramount importance in the preservation and marketing of fresh or processed foods [1]. Among others, petroleum-based packaging materials are extensively used in the food industry field due to their good mechanical and barrier properties as well as their low cost [2]. However, given the growing level of environmental awareness created by excessive plastic accumulation along with consumer requirements for healthy and convenient food products with extended shelf life, several researchers have paid considerable attention to biopolymer-based films and coatings [2]. These packaging systems are produced using biopolymers which are derived from natural and renewable resources [1,3]. Depending on the formulation and the production process, bio-based films can be biodegradable, biocompatible or even edible, which offers new application opportunities. Besides, these films may provide added advantages, namely gas barrier properties and potential applications in food preservation [1,3].

Active food packaging can be developed by enriching biodegradable films with functional additives such as antioxidant compounds, which may migrate from the packaging material to the food product so as to extend the shelf life of food and improve its safety and quality properties [3–5]. Over the past decades, several polysaccharides including starch, cellulose, pectin, chitosan and sodium alginate have been used to produce food packaging [6,7]. Chitosan, for instance, is a cationic polysaccharide composed of randomly distributed β-(1–4)-linked D-glucosamine and *N*-acetyl-D-glucosamine. It is derived by the deacetylation of chitin, which is available in crustacean shells, insects and fungi [1,3]. Compared with other polysaccharides, chitosan has been widely used as a film and a coating material owing to such distinct advantages as its good film-forming and antimicrobial properties. Besides, chitosan-based films have good mechanical and oxygen barrier properties [3].

Although chitosan is a promising biodegradable polymer for producing active packaging films, its low antioxidant and UV-blocking properties as well as its high water solubility can limit the range and effectiveness of its application [8]. Therefore, the incorporation of antioxidant substances into chitosan films may develop innovative materials with enhanced antioxidant properties and maintain food quality and integrity.

Considering the potential health risks associated with the consumption of synthetic additives, recent researches have focused on the integration of natural antioxidants which are not related to toxicological effects, particularly plant extracts and essential oils, into bio-based

packaging materials. Various plant extracts and essential oils including grape seed extract [8], peanut extracts [9], apple peel extract [10], bergamot essential oil [11], citronella essential oil, cedarwood essential oil [2] and *Perilla frutescens* (L.) essential oil [12] have recently been incorporated into chitosan films. These ingredients have been shown to enhance the antioxidant properties of the films. Furthermore, such films have presented changes in terms of techno-functional properties, resulting from the molecular interactions between the film components.

It is crucially important to explore the application of new plant extracts in order to develop active films for food preservation purposes. For instance, *Artemisia campestris* is one of the promising plants due to its interesting biological properties. It is an aromatic herb belonging to the Asteraceae family and is commonly used as an herbal remedy against a variety of diseases in Northern Africa. Its leaves are widely used in Tunisian folk medicine as a decoction for their antispasmodic, anti-inflammatory, antivenom, antirheumatic and antimicrobial activities as well as antispasmodic properties [13]. Numerous works have indicated that the pharmaceutical properties of *A. campestris* including antioxidant, antimicrobial, anti-inflammatory and anti-tumor activities are attributed to the essential oil and polyphenol-rich extracts [13–15]. Other studies have shown that *A. campestris* phenolic extracts and its essential oil exhibited not only an antibacterial activity against food-born pathogenic bacteria but also antifungal properties [15–18]. It is evidenced that *A. campestris* ethanolic extract prevents product spoilage, extends shelf life and improves the quality of vacuum-packed sardine (*Sardina pilchardus*) fillets stored at 3 °C for a period of 21 days [19]. Additionally, the essential oil from the *A. campestris* shoots has been found to protect stored cereal against the damages induced by the grain insect *Tribolium castaneum* [20]. Moreover, *A. campestris* essential oil has been reported as a potential candidate for food preservation against the beetles attacking legumes: *Callosobruchus maculatus* (F.) and *Bruchus rufimanus* [21]. Therefore, *A. campestris* is suitable for preserving food since it can help to extend the shelf life and to prevent various food products from spoilage. However, the direct incorporation of essential oils and phenolic-rich extracts into food matrices can be limited due to their intense flavor that may affect the product acceptance. Hence, it would be interesting to include these ingredients in active packaging to reduce their undesirable effects on the proprieties of foods [22].

A. campestris which is a good source of bioactive components with multiple biological activities has a high potential to serve as an active ingredient that can be incorporated into

films in order to develop new material with desired properties. The aim of the present work is thus to develop chitosan-based films with enhanced functional properties for potential use as antioxidant packaging materials by supplementing natural antioxidants of *A. campestris* including the aqueous and hydroalcoholic extracts as well as the essential oil with chitosan. The effect of *A. campestris* components on the physical, structural, thermal and antioxidant properties as well as on the UV-Vis light barrier was investigated.

2. Materials and methods

2.1. Source of materials

A. campestris was collected in June 2016 in batch in the same sampling area from a naturally growing plant site in Sfax, Tunisia (latitude 34 46′29″N, longitude 10 39′73″E and elevation: 41 m), a region with a semi-arid climate which is characterized by an annual rainfall of 200 mm. After harvest, the plant was air dried for 10 days and the leaves were ground using a mechanical mill (Retsch GM200, Germany). The obtained powder was stored at -20 °C until use. The authenticity of the plant was evaluated in the Laboratory of Analysis, Valorization and Food Safety (National Engineering School of Sfax, Sfax, Tunisia).

Low molecular weight chitosan (150-190 KDa), Product No. 448869) with a deacetylation degree of 75–85 % was purchased from Sigma-Aldrich Company Ltd, United Kingdom. Ferrous chloride, ferric chloride, anhydrous sodium sulfate, quercetin, gallic acid and glycerol were bought from Fluka Chemika (Steinheim, Switzerland). Aluminum chloride, potassium ferricyanide, trichloroacetic acid, potassium phosphate and sodium carbonate were purchased from Suvchem laboratory chemicals (Mumbai, India). Folin–Ciocalteu reagent, sodium chloride and ferrozine (3-(2-Pyridyl)-5,6-diphenyl-1,2,4-triazine) were provided by Loba chemie (Mumbai, India). Tween 80 and DPPH (1-diphenyl-2-picrylhydrazyl) were purchased from Sigma-Aldrich chemie (Steinheim, Germany). Ethanol and glacial acetic acid were bought from Novachim (Tunisia).

2.2. Preparation and analysis of *A. campestris* extracts

2.2.1. Preparation of *A. campestris* aqueous and hydroalcoholic extracts

A. campestris aqueous and hydroalcoholic extracts (ACAE and ACHE respectively) were macerated at 25 °C using water and ethanol-water (80:20, v/v) as solvents. Consequently, *A. campestris* leaf powder (100 g) was suspended in 2 L of each solvent. These mixtures were shaken for 3 h using an orbital shaker and then they were centrifuged at 3000 x

g for 20 min. The obtained supernatants were recovered. The residues were later re-extracted following the same procedure described above. The supernatants of each extract were combined afterward. The evaporation of ethanol present in ACHE was obtained under vacuum at 40 °C using a rotatory evaporator. Finally, ACHE and ACAE were freeze-dried and kept in the dark at 4 °C until analysis. The yield (%, w/dw) of the freeze-dried extracts was calculated as follows:

$$\textit{Yield (\%)} = \frac{W1}{W2} \times 100 \qquad (1)$$

where *W1* is the weight of the extract after freeze drying (g), and *W2* is the weight of the *A. campestris* leaf powder (g).

2.2.2. Determination of total polyphenol and flavonoid contents

The total phenolic content (TPC) of *A. campestris* extracts was measured using the Folin-Ciocalteu method slightly modified by Dewanto et al. [23]. Briefly, 20 µL of the extract was mixed with 100 µL of Folin Ciocalteu reagent. The mixture was homogenized and then incubated for 6 min at room temperature. A volume of 1250 µL of a sodium carbonate solution (7%, w/v) was added and the mixture was vortexed and incubated in the dark for 90 min at room temperature. The absorbance was measured at 760 nm. Gallic acid (GA) was used as a standard for the analytical curve. TPC was expressed in mg of GA equivalents (GAE)/g of the extract.

The total flavonoid content (TFC) of the extracts was determined according to Zhishen et al. [24]. In brief, 250 µL of the extract was mixed with 1 mL of distilled water and 100 µL of a $NaNO_2$ solution at 15 % (w/v). 75 µL of an $AlCl_3$ solution at 10 % (w/v) was added after 6 min. The mixture was later held for 5 min at room temperature. Afterward, 1 mL of NaOH (40 g/L) was added. The solution was then adjusted with distilled water to 2.5 mL. After 15 min, the absorbance was measured at 510 nm. TFC was expressed in mg of Quercetin equivalent (QE)/g of the extract.

2.2.3. Extraction and analysis of *A. campestris* essential oil (ACEO)

The aerial parts of *A. campestris* (500 g) were subjected to hydrodistillation in 5 L of distilled water for 4 h [25]. The EO was separated from the aqueous distillate and collected using a separating funnel. Then, the obtained EO was dried using a small amount of anhydrous sodium sulfate (Na_2SO_4) and was stored in an amber flask at -20°C for further experiments.

The composition of ACEO was conducted by gas chromatography-flame ionization detection (GC-FID) and gas chromatography-mass spectrometry (GC-MS) using an Agilent 6890N GC coupled with an Agilent 5973N MSD. The GC was equipped with HP-5ms 5 % phenyl methylsiloxane capillary column (30.00 m length × 0.25 mm i.d. and 0.25 μm film thickness). The carrier gas was helium at a flow rate of 1.4 mL min^{-1}. The oven temperature program was set at 40 °C and then held for 1 min. Subsequently, it was raised to 200 °C at 5 °C/min and later to 300 °C at a rate of 10 °C/min. Afterward, the temperature was maintained at 300 °C for 5 min. Mass spectra were measured using the electronic impact mode at 70 eV. The retention indices (RI) of all components were determined by comparing their retention times with those of a series of n-alkanes. The identification of ACEO constituents was assessed by comparing their retention indices and mass spectra to the data from the Wiley mass spectral library (275.L) and also to the literature [26]

2.3. Film preparation

Chitosan-based films were produced using the casting method. As a consequence, 2 g of chitosan powder were dissolved in 100 mL of an aqueous solution of glacial acetic acid (1%, v/v). The solution was stirred at 25 °C until complete dissolution. Next, glycerol (0.6 g) was added and the resulting mixture was then magnetically stirred for 30 min to obtain a CH film-forming solution. Subsequently, ACHE (1%, w/v) and ACAE (1%, w/v) were independently dispersed in the chitosan solution.

As for the films enriched with ACEO (1 %, w/v), Tween 80 was added as a surfactant at a level of 0.2 % (v/v) of essential oil [27] and the solution was homogenized using a T 25 ULTRA-TURRAX (IKa WERKE, Germany) at 7500 rpm for 2 min. The amounts of essential oil and the extracts were chosen based on preliminary studies and previous works [22,28]. After the homogenization was complete, all of the dispersions were degassed using an ultrasonic bath for 15 min at room temperature to remove air bubbles [22]. The resulting solutions were cast onto polystyrene Petri dishes and were dried in an oven at 35 °C for 48 h. The dried films were peeled and stored for 72 h or more in a desiccator with saturated NaCl solution (75 % relative humidity) at 25 °C before testing.

The film designations were control (chitosan only), CH-ACHE (chitosan and ACHE), CH-ACAE (chitosan and ACAE) and CH-ACEO (chitosan and ACEO).

2.4. Rheological behavior of film-forming solutions

The rheological behavior of the film-forming solutions (FFS) was measured using a Modular Compact Rheometer MCR 302 (Anton Paar, Austria), equipped with a cone-plate geometry CP50-1(diameter = 50 mm, cone angle = 4°) [29]. The gap between the cone and the plate was 0.102 mm. The measurements were made at 25 °C with the shear rate ranging from 0.01 to 500 s^{-1}.

The power law model (Eq. (2)) was applied to describe the steady shear behavior of the film-forming solutions.

$$\tau = K\gamma^{n} \quad (2)$$

where τ is the shear stress (Pa), K is the consistency index (Pa s^{n}), γ is the shear rate (s^{-1}) and n is the flow index.

2.5. Film characterization

2.5.1. Film thickness

The film thickness was measured with a digital micrometer (Mitutoyo 150 mm, Japan). For each sample, the average of the 5 measurements which were taken randomly at different locations was used to calculate the opacity and the tensile strength (TS).

2.5.2. Determination of moisture content, swelling degree and solubility

The moisture content, the swelling degree and the solubility of the films were determined as described by Bajić et al. [30]. Previously conditioned film specimens (2 × 2 cm^2) were weighed using an analytical balance with a precision of 0.001 mg (Mettler Toledo, Switzerland) referred to as the initial weight (M1). The film samples were then dried in an oven for 24 h at 105 °C to determine the initial dry mass (M2). Film specimens were subsequently placed in beakers containing 30 mL of distilled water and stored for 24 h at room temperature (23 °C ± 2 °C). Next, the films were superficially dried with a filter paper and weighted (M3).

The residual film specimens were later dried for 24 h at 105 °C to get the final dry mass (M4). The water content, the swelling degree and the film solubility were calculated through the following equations respectively:

$$\textit{Water content (\%)} = [(M1 - M2)/M1] \times 100 \quad (3)$$

$$\textit{Swelling degree (\%)} = [(M3 - M2)/M2] \times 100 \quad (4)$$

$$\textit{Solubility (\%)} = [(M2 - M4)/M2] \times 100 \quad (5)$$

2.5.3. Optical properties

2.5.3.1. Color

The measurements of the film color were assessed using a colorimeter CR-5 (Konica Minolta, Europe). Lightness (L*) and chromaticity parameters: a* (red/green) and b* (yellow/blue) were used to characterize the film color in the CIELab coordinate system.
The total color difference (ΔE*) and chroma (C*) were calculated according to the following formula:

$$\Delta E^* = [(\Delta L^*)^2 + (\Delta a^*)^2 + (\Delta b^*)^2]^{1/2} \quad (6)$$

$$C^* = [(a^*)^2 + (b^*)^2)]^{1/2} \quad (7)$$

where ΔL*, Δa*, and Δb* are the differences between the corresponding color parameter of each sample and that of the control film.

2.5.3.2. UV–Vis light barrier and Opacity

The ultraviolet (UV) and visible (Vis) light barrier properties of the films were evaluated using a UV-Vis spectrophotometer (Model UV-2401; Shimadzu, Kyoto, Japan) by scanning the film samples in the wavelength range between 200 and 800 nm. The results were expressed as percent transmittance (%T).

The opacity of the films was determined via the following equation:

$$Opacity\ (mm^{-1}) = -\log T_{600}/e \quad (8)$$

where T_{600} is the fractional transmittance at 600 nm and e is the film thickness (mm).

2.5.4. Fourier transform infrared (FTIR) spectroscopy

The preliminary structures of the chitosan-based films were evaluated using an IRAffinity-1S Fourier transform infrared spectrophotometer (Shimadzu, Japan) equipped with an attenuated total reflectance (ATR) accessory with a diamond crystal. The film sample (1 × 1 cm^2) was placed over the crystal cell and pressed onto the surface using a pressure anvil. The spectra were recorded in the transmittance mode from 400 to 4000 cm^{-1} by averaging 64 scans at a resolution of 4 cm^{-1}. Calibration was performed using background spectrum recorded from the clean and empty cell. The experiments were performed using the LabSolutions IR software (Shimadzu).

2.5.5. X-ray diffraction (XRD)

The X-ray diffraction analysis on chitosan-based films was carried out using a D8 Advance diffractometer (Bruker) with a Cu αK radiation at 40 kV and an incident current of 30 mA. Diffractograms were taken in the 2θ range of 5 - 40° with a scan rate of 2 °/min.

2.5.6. Scanning electron microscopy (SEM)

The surface and cross-section morphologies of chitosan-based films were observed using a scanning electron microscope (Thermo Scientific Q250). Prior to observation, samples were cut (5 × 5 mm²) and fixed on a multi stub holder using a double-sided adhesive tape [31]. The images were taken at a low vacuum mode with an absolute pressure of 70 Pa and an accelerating voltage of 15 kV.

2.5.7. Thermogravimetric analysis (TGA)

The thermal stability of the films was determined using a thermogravimetric analyzer (TGA/DSC 1 star system, Mettler Toledo, Greifensee, Switzerland). The weight change of each film sample (10 mg) was recorded throughout heating from 30 to 600 °C at a heating rate of 10 °C/min under a constant nitrogen flow (35 mL/min) to avoid thermo-oxidative reactions.

2.5.8. Mechanical properties

The mechanical properties of chitosan-based films including the tensile strength (TS) and the elongation at break (EAB) were determined according to the Standard Test Method ASTM D882 [32]. Experiments were carried out using a Texture analyzer (TA-XT2i, Stable Micro Systems, United Kingdom) with a cell load 100 N equipped with tensile grips. Film strips (70 × 20 mm²) were fixed in the film-extension grips with an initial grip separation of 50 mm and then stretched at 50 mm/min of crosshead speed until breakage [22].

TS (MPa) and EAB (%) were obtained by the Eqs. (9) and (10) respectively:

$$TS = F_{max} / (W \times x) \quad (9)$$

where F_{max} is the fracture stress of the films (N), W is the film width (mm), x is the film thickness (mm).

$$EAB = (\Delta L / L_0) \times 100 \quad (10)$$

where ΔL is the film elongation when it was broken (mm), and L is the initial length of the film (mm)

2.5.9. Antioxidant capacity of chitosan-based films

2.5.9.1. DPPH radical scavenging assay

The radical scavenging activity of the films was determined using the DPPH (2,2-diphenyl-1-picrylhydrazyl) assay according to Byun, Kim et al. [33] with minor modifications. Approximately 100 mg of each film sample was cut into small pieces and dissolved in 10 mL of ethanol (95 %, v/v) for 2 hours. One aliquot (500 µL) of each film extract was mixed with 375 mL of ethanol (95 %, v/v) and 125 µL of an ethanolic solution of DPPH at 0.02 % (w/v). The solution was kept in the dark at room temperature for 1 hour. Absorbance was measured at 517 nm using a UV–Vis spectrophotometer.

DPPH radical scavenging activity was calculated through the following equation:

$$\textbf{Scavenging activity (\%)} = [(A0 - Ab - As)/A0] \times 100 \quad (11)$$

where A_0 is the absorbance of the control reaction, A_s is the absorbance of the sample and A_b is the absorbance of the blank mixture.

2.5.9.2. Reducing power assay

The reducing power of the films was determined according to Yildirim et al. [34]. As a result, 0.5 mL of each film extract was mixed with 1.25 mL of phosphate buffer (0.2 M, pH 6.6) and 1.25 mL of a potassium ferricyanide solution (1%, w/v). The mixtures were incubated for 30 min at 50 °C. After incubation, 1.25 mL of trichloroacetic acid (10 %, w/v) was added and the reaction mixtures were then centrifuged for 5 min at 3000 x g. The supernatant (1.25 mL) was mixed with 1.25 mL of distilled water and 0.25 mL of ferric chloride ($FeCl_3$, 0.1 %, w/v). The mixtures were kept in the dark for 10 min and the absorbance of the reaction mixture was measured at 700 nm. Increased absorbance of the reaction mixture indicated an increase in the reducing power.

2.5.9.3. Ferrous ion chelating ability assay

The chelating effect of the films on ferrous ions (Fe^{2+}) was determined according to Dinis et al. [35]. Briefly, 50 µL of $FeCl_2$ of 2 mM were added to 500 µL of each film extract. The mixtures were incubated at room temperature for 15 min. Subsequently, the reactions were triggered through the addition of 100 µL of 5 mM of a ferrozine solution (3-(2-Pyridyl)-

5,6-diphenyl-1,2,4-triazine). The mixtures were then shaken vigorously and kept at room temperature for 30 min. The control tube was prepared in the same manner by substituting the film solution with water. The absorbance of the solutions was subsequently recorded at 562 nm and the percentage of inhibition of ferrozine-Fe^{2+} complex formation was calculated using the following equation:

$$\textit{Metal chelating activity (\%)} = [(Ac - Ae/Ac)] \times 100 \quad (12)$$

where A_c and A_e represent the absorbance of the control and the sample reaction respectively.

2.6. Statistical analysis

All experiments were done in triplicate at the very least. The experimental results were presented as mean ± standard deviation. Data evaluation was carried out by the statistical analysis software IBM SPSS Statistics 21. Differences between samples were evaluated using the Duncan's Multiple Range test ($p < 0.05$).

3. Results and discussion

3.1. Chemical composition of *A. campestris* essential oil

The general chemical composition of the *A. campestris* essential oil is presented in Table 1. The ACEO revealed the presence of 21 major compounds representing 98.94 % of the total oil. The main components were β-pinene (25.67 %), limonene (15.39 %) and γ-terpinene (10.48 %) forming 51.51 % of the total oil. The most dominant chemical group was monoterpene hydrocarbons (88.01 %). These chemical compounds were involved in the antioxidant and antibacterial properties of ACEO as well as other plant extracts and essential oils [13,14,36]. Our results on the chemical profiling of the ACEO are in line with the study performed by Akrout et al. [14] where the main compounds of ACEO were also β-pinene (34.2 %), limonene (8.2 %), D-germacrene (7.3 %), γ-terpinene (6.1 %), β-myrcene (6.0 %) and α-pinene (5.3 %). However, several studies reported different chemical profile of ACEO [25,37]. The variations in the chemical composition of ACEO might be due to the different geographical and climate conditions, the variety of species, the extraction process and the phenological stage [38].

3.2. Total phenolics and flavonoids of *A. campestris* extracts

The extraction yields, the total phenolic and flavonoid contents are presented in Table 2. The extraction yield of ACHE (16.81 %) was higher than that of ACAE (13.17 %). The total phenol and flavonoid contents in ACAE were 101.19 mg GAE/g of the extract and 79.80 mg QE/g of the extract respectively. ACHE, by contrast, had higher total phenol and flavonoid contents (269.98 mg GAE/g of the extract and 195.12 mg QE/g of the extract respectively). Similarly, Megdiche-Ksouri et al. [15] reported that *A. campestris* extracts contain a considerable amount of phenolic compounds, being higher for the ethanolic extract in comparison with the aqueous extract.

3.3. Rheological behavior of film forming solutions: steady shear measurements

It is important to investigate the rheological properties of the casting solutions of the bicomponent films to control their manufacturing process [39]. The experimental flow curves for different film-forming solutions are presented in Figure 1 which shows that the viscosity of all FFS was shear-rate dependent since it decreased with the increase in the shear rate, reflecting a shear-thinning behavior. In fact, when the shear rate increased, the molecules that were entangled with each other lined up in the direction of the flow. Therefore, fewer interactions occurred within polymer chains, leading to a decrease in the apparent viscosity [40]. A similar behavior has been reported for control chitosan and chitosan composite FFS [28,29,41].

Rheological data were fitted to the power law model. The model parameters are depicted in Table 3 together with the apparent viscosity (η_{ap}) values at the shear rates of 0.1 s^{-1} and 100 s^{-1}. The shear thinning nature of FFS has been confirmed as the flow behavior index (n) values were lower than 1 for all the samples. Meanwhile, this behavior was less pronounced for the FFS enriched with ACHE and ACEO since their n value was significantly higher ($p < 0.05$). Thus, the behavior of these solutions was closer to Newtonian fluids, indicating a lower influence of the shear rate on the viscosity [42]. The incorporation of *A. campestris* antioxidants also induced a decrease in the consistency index (k) and the apparent viscosity. Besides, a comparatively strong effect was observed in the case of CH-ACAE FFS, resulting in a very low viscosity solution. The reduction in the apparent viscosity of FFS added with extracts could be due to the weak hydrogen bonding within polymer chains, resulting from the interaction between polyphenols and chitosan. Moreover, the difference in viscosity between CH-ACHE and CH-ACAE FFS could be ascribed to the different compositions of each extract [9]. Comparatively, Peng et al. [28] reported the same behavior

when chitosan FFS were enriched with tea extracts. The changes of the rheological behavior in chitosan films mixed with ACEO might be attributed to the fact that the chitosan concentration in the continuous phase shifted as a result of its adsorption at the oil-water interface. This was probably due to the modifications in the net electric charge of the particles [43]. A similar behavior of chitosan FFS containing bergamot EO and thyme EO was reported [11,44].

3.4. Physical properties of the films

3.4.1. Thickness

The film thickness values ranged from 0.134 to 0.21 mm (Table 4). Significant differences ($p < 0.05$) were observed when comparing the control film with films containing *A. campestris* extracts. Indeed, the addition of ACAE to the chitosan matrix led to a decrease in the film thickness while an increase in the film thickness was noticed when adding ACHE and ACEO. The nature of the film-forming polymer and the content of the additives affected the film thickness due to their interactions within the polymer matrix [45,46]. In CH-ACHE films, interactions between ACHE polyphenols and chitosan possibly took place, including hydrogen bonding and hydrophobic forces [47]. Therefore, the organized structure of the film matrix was interrupted by the extract components. This triggered an increase in the spatial distance within the chitosan matrix and consequently a greater thickness [48]. The enhanced solid content in the CH-ACHE film could also promote the increase in the film thickness. The reduction in film thickness resulting from the addition of ACAE could, by contrast, be ascribed to the reduction in the obstruction of the molecular chain and the drastic decrease in the viscosity of film-forming solutions [9]. In this context, Meng et al. [9] reported that peanut shell extracts decreased film thickness while the peanut skin extract did not affect it. Additionally, Sun et al. [49] found that supplementing apple polyphenols with chitosan films led to an increase in the film thickness. As regards the films enriched with ACEO, the increase in the thickness could result, among other things, from the increased porosity of the films. It has also been shown that the different chemical constituents of essential oils such as α-pinene, myrcene and limonene could interact with chitosan films in different ways, which led to an increase in the volume of the film [38]. A similar effect of cinnamon EO on the chitosan film thickness has been reported by Ojagh et al. [50]. However, Shen and Kamdem [2] found that the incorporation of citronella and cedar essential oils did not have any significant effect on the thickness of chitosan films.

3.4.2. Water content, water solubility and swelling degree of the films

The changes in the water content, the water solubility and the swelling degree of the composite films are shown in Table 4. The water content is a parameter linked to the total free volume occupied by the water molecules in the film network. The control film exhibited the highest water content value (36.09 %). The moisture content of CH-ACHE and CH-ACAE films decreased significantly (26.34 and 27.46 % for CH-ACHE and CH-ACAE respectively) compared to the control film. These findings suggest that the polyphenols of ACHE and ACAE could interact with the OH and NH_2 groups of chitosan via hydrogen and/or covalent bonds, which limits the availability of the CH functional groups to water. Similar results were observed by Zhang et al. [51] and Yang et al. [47] for chitosan films enriched with the phenolic extract of mangosteen and the syringic acid respectively. Following the addition of ACEO, the moisture content of the film also decreased (30.49 %) but the effect was lower than that of ACHE and ACAE. The reduction in water content of the CH-ACEO could be due to the increase in the hydrophobicity of the films. It has been reported that interactions could occur between the essential oils and the functional groups of chitosan, which brought about a decline in the availability of hydroxyl and amino groups, thereby limiting the interaction between the polysaccharide and water through hydrogen bonding. Additionally, covalent bonds were found to occur between essential oils and chitosan matrix leading to a decrease in the water affinity of the film [52].

Water solubility is an essential characteristic of films used for food packaging. This property reflects the water resistance and the biodegradability of the films [53]. The solubility could provide information about the possibility of releasing the active substances contained in the films when contacting the food surface [27]. Water resistance or insolubility is generally recommended for the potential application of biodegradable food films, especially in humid environments [53]. The water solubility of the control chitosan film was 18.30 %. The addition of ACEO to the chitosan film resulted in a significant decrease in the film solubility (12.80 %) due to the hydrophobic nature of the EO. Haghighi et al. [53] reported that chitosan and the gelatin composite film showed a significant decrease in the solubility of films when incorporated with nutmeg essential oil, whereas the films enriched with thyme and cinnamon essential oils demonstrated a substantial increase in the film solubility. They suggested that these differences are related to the hygroscopic properties of these essential oils, which are involved in the attraction of water molecules and in the ability to establish polymer-oil interactions that weaken the interactions between chitosan and gelatin. The incorporation of

ACHE reduced the solubility of the films while the addition of ACAE resulted in a considerable increase in the solubility of the CH-ACAE film. The differences in the solubility of the CH-ACAE film and the CH-ACAE film are related to the variation in the hydrophobicity of the extracts. Indeed, the rise in the solubility of the CH-ACAE film was attributed to the hydrophilic nature of ACAE while the decreased solubility of CH-ACHE was due to the hydrophobic character of ACHE. Similarly, Peng et al. [28] noted that the solubility of chitosan films significantly increased when green tea and black tea extracts were added to the film.

The swelling degree is a parameter linked to the degree of crosslinking that occurred in the polymer network, thereby affecting the water resistance of the film. The lower the swelling degree of polymeric films is, the higher the water resistance of the film is [5]. The swelling index of the control chitosan films is 88.28 % as shown in Table 4. The high swelling value was ascribed to the hydrophilic character of chitosan. The incorporation of ACEO did not have a significant effect on the swelling properties of chitosan films. On the contrary, the enrichment of the films with the extracts of *A. campestris* caused a significant decrease in the swelling degree which is particularly noticeable for ACAE. The decline in the swelling degree of CH-ACAE and CH-ACHE films in comparison with the control film could be due to the reduction in the free volume in the polymer network. Besides, the changes in the swelling degree could be related to the interactions between chitosan and polyphenols, which made the swelling degree of the enriched films lower than the control film. It should also be taken into consideration that dry films were used for the determination of the swelling degree and the solubility of the films. Hence, crosslinking could take place between the chitosan and the polyphenols under the effect of temperature (105 °C), which led to the reduction in the interaction between chitosan and water via hydrogen bonds [30,54]. In their study, Mayachiew and Devahastin [54] reported that, when enriched with amla extract, the degree of swelling of the chitosan film decreased and that this parameter depended on the drying method of the films. In fact, they found that due to temperature-induced crosslinking, the swelling degree went down as soon as the drying temperature climbed. In this context, Di Pierro et al. [55] reported that the swelling degree of polymer films strongly depended on the amount and the nature of the intermolecular chain interactions.

The overall observations showed that CH-ACHE and CH-ACEO films presented an improved water resistance, implying their potential use as active food packaging materials that protect food, especially in humid environments.

3.5. Optical properties

3.5.1. Color and opacity

The color and the opacity of the packaging film are important factors for general appearance and consumer acceptance. The color parameters (L*, a*, b*, ΔE*, C*) and the opacity values of different films are presented in Table 5 which shows that the chitosan film was transparent and exhibited a light yellow color. The incorporation of ACEO in chitosan films led to a slightly more yellowish appearance (higher values of b*) and more opaque films ($p < 0.05$). The increased opacity of CH-ACEO films might be due to the light scattering provoked by lipid droplets inserted into the chitosan chains [56]. A significant change in film color and opacity was observed when *A. campestris* extracts were added ($p < 0.05$). In fact, the addition of ACHE and ACAE induced a decrease in film lightness and a color shift towards red (+a*) and yellow (+b*) as well as an increase in the film opacity ($p < 0.05$). These films also showed a more saturated color since the chroma (C*) increased. These differences might be attributed to the inner color of the extracts due to the presence of phenolic compounds and pigments [57]. The increase in the opacity of the films enriched with extracts could be ascribed to the higher saturated color of the films. Similar results were reported for chitosan films when supplementing the green tea extract and the ginger essential oil [22,58]. In line with our results, it has been demonstrated that the green tea extract and the mangosteen extract induced a significant change in the color and a significant decrease in the transparency of the chitosan films [31,58].

3.5.2. UV-Vis light barrier

UV-Vis light barrier is a desired characteristic for food packaging materials since the exposure to visible and ultraviolet lights may induce oxidative deterioration of food resulting in nutrient losses, discoloration and off-flavors [31]. Thus, the light barrier properties of chitosan-based films were characterized by the light transmittance in the range of 200-800 nm and the resulting spectra are presented in Fig. 2. The latter shows that UV-Vis transmittance of chitosan films was considerably reduced when *A. campestris* active compounds were incorporated. Indeed, the light transmittance values in the UV range (≤ 400 nm) for the control chitosan films were ranging from 0 % to 57 %, whereas the films enriched with ACEO had lower transmittance values ranging from 0 % and 14 %. Besides, the UV transmittance of CH-ACAE and CH-ACHE films was almost zero which indicates a complete

blockage of the UV light transmittance for these films. This was probably due to the strong ability of the polyphenols present in the extracts to absorb UV light [51,57].

On the other hand, the light transmittance of the control film in the visible domain reached 80 % while the maximum transmittance values for films enriched with ACEO, ACHE, and ACAE were reduced by 30, 12 and 55 % respectively. The phenolic extracts of *A. campestris* showed various effects on the visible light transmission. This could be attributed to the amount, the nature and the distribution of phenolic compounds in the film matrix which led to different film morphologies with different light transmission. In fact, ACHE had higher content of total phenolics and flavonoids. These films presented a higher visible light barrier. Our results suggest that the films added with *A. campestris* antioxidants improved the UV-Vis light barrier as compared with the control film. Similarly, Souza et al. [22] found that several plant essential oils and especially hydroalcoholic extracts improved the light barrier of chitosan films.

The composite films could be further selected to produce food packaging materials having the ability to block the most damaging light wavelengths and consequently prevent the formation of toxic substances, off-odors and off-flavors as well as the food color loss and the photo-oxidation of lipids.

3.6. Structural properties

3.6.1. FTIR Analysis

The Fourier transform infrared spectroscopy was performed to assess the intermolecular interactions between the functional groups of chitosan and the constituents of *A. campestris* extracts and essential oil. These interactions are related to the physical and the mechanical performances of the blend films. All film samples exhibited almost a similar FTIR spectral pattern presenting mainly the characteristic peaks of chitosan (Fig. 3).

The spectrum of the CH film showed characteristic bands of amide I (1639 cm^{-1}), amide II (1547 cm^{-1}) and amide III (1318 cm^{-1}). The broad band observed at 3264 cm^{-1} was assigned to the O-H stretching vibrations which overlapped with the N-H stretching vibrations [57]. The peaks at 2924 and 2872 cm^{-1} were assigned to the C-H stretching vibrations related to the pyranose ring [28]. The spectrum also showed peaks at 1151, 1067 and 1027 cm^{-1} corresponding to the asymmetric stretching of the C-O-C bridge, C-O stretching and glycosidic linkage respectively [59].

The incorporation of ACEO into the chitosan films did not reveal a noticeable change in the FTIR pattern except a slight shift of the band at 3264 cm^{-1} and then became flatter. This indicates the occurrence of hydrogen bonds between O-H groups in the oil components and the N-H and O-H groups in chitosan. These results are in line with those reported by Shen and Kamdem [2] for the chitosan film enriched with citronella essential oil.

When ACAE was incorporated into the chitosan matrix, the characteristic band at 1547 cm^{-1} (amide II) moved to a higher wavenumber, whereas the band at 1318 cm^{-1} (amide III) shifted to a lower wavenumber and became less discernible. This was due to the molecular interaction between the phenolic compounds in ACAE and the amino functional groups. Since the intensity of amide bands did not change and no new peak appeared, the occurrence of interactions between ACAE and chitosan was likely via non covalent bonds.

After the incorporation of ACHE in the CH film, significant changes were observed in the FTIR spectrum. In fact, Fig.3 shows a movement of the peak related to amide I to a lower wavenumber and a decrease in the intensity of the chitosan characteristic peaks (amide I, amide II and amide III). It was also noted that the addition of ACHE into the chitosan matrix revealed the appearance of weak peaks at 1267 cm^{-1} and between 930-650 cm^{-1} which were attributed to the O-H bending vibration of the polyphenols and to the deformation vibrations of C-H in the benzene ring respectively [60]. Besides, the absorption band at 3264 cm^{-1} moved to a lower wavenumber and became more flattened. These findings suggest the formation of intermolecular interactions between the hydroxyl and amino groups of chitosan and the functional groups of the phenolic compounds of ACHE via hydrogen bonds as well as covalent bonds. The functional groups of chitosan were thereby occupied and the free hydrogen groups which could form hydrophilic bonding with water thus decreased. This may explain the weakened solubility and water content of CH-ACHE films as it was described in a previous section.

Intramolecular and intermolecular interactions between chitosan and incorporated plant extracts via Hydrogen bonding were reported in the literature [5,7,10,49]. Moreover, Liu et al. [4] as well as Siripatrawan and Harte [58] have reported that, through covalent bonds, chitosan interacted with protocatechuic acid and green tea extracts respectively.

3.6.2. X-ray diffraction (XRD) analysis

The XRD analysis was performed to evaluate the change in the crystalline and the amorphous structure of blend films. The diffractograms of different films are shown in Fig. 4. The control chitosan film exhibited five diffraction peaks at around 2θ = 8.24, 11.26, 16.15, 17.94 and 23.65°. This suggests the semicrystalline character of the film which confirms previous studies [61,62]. The peaks at 2θ = 8.24 and 11.26° were attributed to the hydrated crystalline structure resulting from the introduction of water molecules in the crystal lattice while the diffraction peak at 2θ = 23.65° was ascribed to the amorphous structure of the chitosan films [4,63].

As it could be seen, chitosan films enriched with various *A. campestris* antioxidants exhibited a different XRD pattern compared with the control chitosan films. In fact, the introduction of ACHE induced a decrease in the intensity of diffraction peaks and led to the appearance of a new weak peak at 9.4°, indicating that the extract was successfully added to the chitosan matrix. Moreover, the incorporation of ACAE in the films revealed a higher effect on the crystalline structure of chitosan films as the pics at 2θ = 8.24, 11.26 and 16.15° disappeared. Therefore, both extracts reduced the crystallinity of the Chitosan films. This might be due to the interaction that occurred between chitosan and *A. campestris* polyphenols which led to a loss of the intermolecular hydrogen bonding of chitosan [4]. It is noteworthy that the differences in XRD patterns of CH-ACHE and CH-ACAE were on account of the different phenolic composition and thereby the different molecular arrangement of the film components. A similar decrease in the crystallinity of chitosan films was noted by Zhang et al. [64] when incorporating different plant extracts. However, after ACEO was added into chitosan films, only the sharp peak at 11.2° was maintained, whereas a broad diffraction peak appeared at around 20° corresponding to the amorphous region. Thus, ACEO induced a considerable decrease in the crystallinity of the chitosan films resulting from the disruption of the original structure of the chitosan molecules due to newly formed intermolecular interactions. Similarly, Valenzuela et al. [65] reported that the addition of sunflower oil to the chitosan-quinoa protein composite films induced a less crystalline structure. Zhang et al. [12], by contrast, reported that the crystalline structure of the chitosan films was enhanced by incorporating the essential oil of *Perilla frutescens* (L.) Britt. This disparity could be due to the differences in the experimental conditions as well as the composition of the film-forming solutions and formulations such as the types of plasticizers and/or polymers and the additives used in the film-forming solutions [66].

3.6.3. Film microstructure

The film microstructure is influenced by the structural arrangement of the different components in the initial dispersion and their behavior during the drying process. Scanning electron microscope (SEM) micrographs of the surfaces and the cross sections of the films are depicted in Fig. 5. The control chitosan films presented a compact and relatively homogenous structure without any pores or cracks. Besides, the film surface was smooth and flat. This was due to the strong hydrogen bond interactions within chitosan molecules [4]. When *A. campestris* extracts were added to the chitosan film, relevant differences in the film microstructure were noticed.

On the one hand, the surface morphology of the films was affected by the incorporation of ACHE and ACAE. When compared to the control film, CH-ACHE and CH-ACAE films presented some white spots on their surfaces which correspond to the phenolic aggregates [10]. The CH-ACHE film particularly showed a rougher surface than that of the CH-ACAE film. The cross-sectional observations also revealed that CH-ACHE and CH-ACAE films had a more heterogeneous and less compact structure. The change in the microstructure of chitosan films after the incorporation of the extracts was attributed to the formation of new interactions between chitosan and phenolic compounds as well as the alteration of the original molecular interactions in the chitosan matrix. Similar observations have been reported for chitosan films enriched with the grape seed extract [31] and the mangosteen extract [51].

On the other hand, CH-ACEO showed, in the cross section of the film, a porous structure which is related to the entrapped oil particles (or their voids) in the continuous polymer network. The oil droplets were quite homogeneously distributed across the film, indicating the absence of creaming and coalescence during drying [67]. This could be related to the stability of the chitosan/essential oil emulsions. As deduced from the measurements of flow behavior, the incorporation of ACEO in chitosan film-forming solutions made the fluid system less viscous and less shear thinning than the solution of the control chitosan film. This behavior was consistent with the adsorption of the chitosan molecules on the droplet surface, which led to reduce their viscous contribution in the continuous phase. Hence, the EO droplets were more stable and more resistant to changes induced by the shear forces that occurred during the aggregation of polymer chains when the solvent evaporated [56,67]. Similarly, Sánchez-González et al. [67] and Perdones et al. [68] reported a sponge-like structure of the chitosan films enriched with lemon essential oil and tea tree essential oil

respectively. However, Ojagh et al. [50] developed chitosan films enriched with cinnamon essential oil and observed sheet-like structures which were stacked in compact layers.

3.7. Thermal stability

The thermogravimetric analysis was carried out in order to evaluate the effect of *A. campestris* active compounds on the thermal stability of chitosan films. The weight loss (TG) and the first derivative (DTG) curves of the different films are shown in Fig. 6. The corresponding degradation temperatures of the films (Td, Tmax, and Tf), weight loss (Δw) and percentage of the residue are depicted in Table 6. As it is shown in Fig. 6 (A, B), the developed films showed three main degradation steps between 30 and 600 °C. The first step (70-130 °C) corresponds to the volatilization of both adsorbed water and residual acetic acid [69]. The second step (110-230 °C) could be ascribed to the degradation of glycerol, structurally bound water and *A. campestris* extracts as well as its essential oil [69,70]. The third step (230-400 °C) accords with the greatest weight loss and is related to the degradation of the chitosan backbone [59].

It is obvious that the thermal degradation profile of the various films presented slight changes with the incorporation of *A. campestris* components. Indeed, when ACEO was added to the chitosan films, the rate of the weight loss and temperature in the first stage declined from 3.78 % to 2.5 % and from 127 °C to 99 °C respectively. These observations might be due to the presence of hydrophobic compounds that decreased the water content inside the film network [7]. Moreover, CH-ACHE and CH-ACEO showed an additional peak at 438 and 365 °C respectively. This could be associated with the residual aromatic compounds present in ACHE and ACEO, which were embedded in the chitosan network. Similar results were reported by Jahed et al. [70], Shen and Kamdem [2] and Zheng et al. [7]. The incorporation of natural antioxidants from *A. campestris* did not notably affect the thermal stability of the chitosan films. Interestingly, all the developed films demonstrated a great thermal stability since the degradation occurred above 300 °C. In this context, Nguyen et al. [5] reported that the thermal stability of chitosan films was not affected by the addition of *Sonneratia caseolaris* (L.) Engl. leaf extract. Meanwhile, Shen and Kamdem [2] showed that citronella essential oil and cedarwood oil slightly enhanced the thermal stability of the chitosan films.

3.8. Mechanical properties

The mechanical properties reflect the durability of the films and their ability to maintain the integrity of packaged food products during handling and storage [38]. The tensile strength (TS) and the percentage of elongation at break (EAB %) of all the prepared films referring to the mechanical properties are presented in Table 4.

The results showed that the mechanical properties of the composite films depended on the type of the added extract. Indeed, when ACEO was supplemented with chitosan films, the tensile strength slightly decreased ($p > 0.05$), whereas the EAB went down by 27 % in comparison with the control films. The incorporation of ACHE induced a decrease in the tensile strength of chitosan films ($p < 0.05$). As regards the CH-ACAE film, the tensile strength drastically fell. Similarly, a significant reduction in the EAB was observed (85 % compared to CH film).

The tensile properties of films depend on various factors including the film constituents, their relative proportions, their interactions as well as the microstructural characteristics of the material [71]. In CH-ACEO, the decrease in EAB could be related to the structural arrangement of the lipid phase into the chitosan matrix. Indeed, the SEM observations of these films showed a porous structure, caused by oil droplets, which induced a loss of film cohesion. This probably led to the creation of rapture points which was related to the decrease in film extensibility. In this context, Moradi et al. [8] reported a reduction in chitosan film extensibility and tensile strength after the incorporation of *Zataria multiflora* essential oil, which was attributed to a rise in pore sizes of the films. On the contrary, Shen and Kamdem [2] found that the enrichment of chitosan films with cedarwood essential oil led to a decrease in TS and an increase in the stretchability of the film. The decline in TS induced by the addition of ACAE and ACHE could be due to the agglomeration of the extracts, which disrupted the homogeneity and the compactness of the film network. The marked decrease in TS and EAB in CH-ACAE film could be the result of the breakage in film network by polyphenols [72]. It has been reported that supplementing polyphenol-rich extracts with chitosan films generally reduces the mechanical properties [6,28,67]. However, the incorporation of phenolic acids has been found to enhance these properties [4,47]. The decline in the mechanical properties in all of the blend films could be also explained by the decrease in the crystalline structure and intermolecular hydrogen bonding in the chitosan network [6,10]. To sum up, the effect of the addition of plant extracts and essential oils on the tensile properties of the films is variable and dependent on the specific interactions within the polymer matrix, which varies according to the type of the extract used.

The overall results showed that supplementing *A. campestris* active ingredients with chitosan films resulted in different types and levels of modifications in both structural and physical properties according to the type of the extract. The incorporation of ACHE in chitosan films caused a decrease in the solubility, in the swelling degree and in the tensile strength. This could be related to the strong interactions between ACHE polyphenols and chitosan matrix. The decrease in TS in CH-ACHE and CH-ACAE films might also be associated with the heterogeneity of the film microstructure and thereby the alteration of the compactness of the films. In the CH-ACAE film, the drastic decrease in TS and EAB was assigned to the breakage in film network by polyphenols. The enrichment of chitosan films with ACEO induced a reduction in the film extensibility. This was due to the porous structure, created by oil droplets that likely caused rupture points. CH-ACEO films showed a decrease in the film solubility on account of the hydrophobicity of ACEO, whereas the swelling degree remained high. This could result from the increased porosity and free volume inside the film. The enriched films demonstrated an increased light barrier. CH-ACHE and CH-ACAE, in particular, exhibited a complete blockage of UV light owing to the strong absorption ability of the polyphenols present in the extracts in the UV region.

3.9. Antioxidant film properties

Antioxidant packaging which is a major part of active packaging is highly promising for increasing the shelf life of products [28]. The antioxidant activities of chitosan films in the presence of different *A. campestris* active components were assessed by three *in vitro* assays with different antioxidant mechanisms: The DPPH radical scavenging assay, the iron-chelating effect and the reducing power assay. The results are depicted in Fig. 7. The control chitosan films exhibited a slight antioxidant activity (10.71 %, 6.38 % and 0.132 for DPPH radical scavenging activity, chelating activity and reducing power respectively) regardless of the test used. The DPPH radical scavenging activity of the chitosan films could be attributed to the ability of the amino groups of chitosan (NH_2) to react with free radicals, generating stable macromolecular radicals and ammonium groups (NH^{3+}) [8].

Overall, the composite films presented a significantly improved antioxidant activity compared with the CH film. This antioxidant activity depended on the type of the incorporated additive. The CH-ACHE film showed the highest DPPH radical scavenging activity, chelating effect and reducing power which were 96.79 %, 54.31 % and 0.272 respectively.

When ACAE and ACEO were added to the CH film, the enhanced DPPH radical scavenging activity and metal chelating ability were observed and greater properties were noted for CH-ACAE. The antioxidant properties of the films enriched with ACHE and ACAE could be attributed to the presence of bioactive compounds including phenolic acids and flavonoids in the extracts. Previous studies reported that the antioxidant activities of *A. campestris* extracts correlate with the amounts of phenolic and flavonoid compounds [15,16]. ACHE had higher total phenolic and flavonoid contents than ACAE, leading to the difference in antioxidant activities of the corresponding films. It has been demonstrated that the antioxidant capacity of *A. campestris* extracts arises from the high reactivity of their compounds as electron donors and also from the ability of the polyphenols to stabilize the unpaired electron and redox properties [15,73]. In CH-ACEO film, the free radical scavenging ability could be related to the high content of monoterpene hydrocarbons and especially the γ-terpinene which is reported as a potent radical scavenging substance [38,74].

4. Conclusion

The novel active films based on chitosan and enriched with *A. campestris* antioxidant extracts and essential oil were successfully developed in the present work. The enrichment of chitosan films with compounds of *A. campestris* led to a great improvement in the antioxidant properties. Chemical interactions between chitosan and different *A. campestris* active ingredients occurred and affected the inner structure of the film and subsequently their physical and mechanical properties depending on the type of the extract. Interestingly, the addition of ACHE and ACEO to the film induced a notable enhancement in the water resistance. Furthermore, a higher light barrier of the blend films was observed, which might improve the ability of the film to prevent lipid oxidation in foods. The addition of ACHE and ACAE in the chitosan matrix decreased the tensile strength. The film extensibility was also reduced when incorporating ACAE and ACEO. The tensile properties of the composite films could be further enhanced through cross-linking treatments. The overall results showed that chitosan films enriched with the antioxidant compounds of *A. campestris* could be formulated for application as alternative food packaging materials. Nevertheless, before their use, further studies are needed on their water vapor permeability, gas barrier properties, release of active compounds etc.

Conflict of interest

The authors have no declared conflict of interest.

Acknowledgements

This work was supported by the Tunisian Ministry of Higher Education and Scientific Research and also by Wallonie-Bruxelles International (WBI) in Belgium. We would like to express our thanks to Ms. Sabriya Mbarek, an English Language Teacher at the Faculty of Science - Sfax, Tunisia for proofreading this paper.

References

[1] S. Kumar, A. Mukherjee, J. Dutta, Chitosan based nanocomposite films and coatings: Emerging antimicrobial food packaging alternatives, Trends Food Sci. Technol. 97 (2020) 196–209.

[2] Z. Shen, D.P. Kamdem, Development and characterization of biodegradable chitosan films containing two essential oils, Int. J. Biol. Macromol. 74 (2015) 289–296.

[3] M.Z. Elsabee, E.S. Abdou, Chitosan based edible films and coatings: A review, Mater. Sci. Eng. C. 33 (2013) 1819–1841.

[4] J. Liu, C. guang Meng, Y. hua Yang, Y. na Shan, J. Kan, C. hai Jin, Protocatechuic acid grafted onto chitosan: Characterization and antioxidant activity, Int. J. Biol. Macromol. 89 (2016) 518–526.

[5] T.T. Nguyen, U.T. Thi Dao, O.P. Thi Bui, G.L. Bach, C.N. Ha Thuc, H. Ha Thuc, Enhanced antimicrobial activities and physiochemical properties of edible film based on chitosan incorporated with *Sonneratia caseolaris* (L.) Engl. leaf extract, Prog. Org. Coatings. 140 (2020) 105487.

[6] S.A. Mir, B.N. Dar, A.A. Wani, M.A. Shah, Effect of plant extracts on the techno-functional properties of biodegradable packaging films, Trends Food Sci. Technol. 80 (2018) 141–154.

[7] K. Zheng, S. Xiao, W. Li, W. Wang, H. Chen, F. Yang, C. Qin, Chitosan-acorn starch-eugenol edible film: Physico-chemical, barrier, antimicrobial, antioxidant and structural properties, Int. J. Biol. Macromol. 135 (2019) 344–352.

[8] M. Moradi, H. Tajik, S.M. Razavi Rohani, A.R. Oromiehie, H. Malekinejad, J. Aliakbarlu, M. Hadian, Characterization of antioxidant chitosan film incorporated with Zataria multiflora Boiss essential oil and grape seed extract, LWT - Food Sci. Technol. 46 (2012) 477–484.

[9] W. Meng, J. Shi, X. Zhang, H. Lian, Q. Wang, Y. Peng, Effects of peanut shell and

skin extracts on the antioxidant ability, physical and structure properties of starch-chitosan active packaging films, Int. J. Biol. Macromol. 152 (2020) 137–146.

[10] A. Riaz, S. Lei, H.M.S. Akhtar, P. Wan, D. Chen, S. Jabbar, M. Abid, M.M. Hashim, X. Zeng, Preparation and characterization of chitosan-based antimicrobial active food packaging film incorporated with apple peel polyphenols, Int. J. Biol. Macromol. 114 (2018) 547–555.

[11] L. Sánchez-González, M. Cháfer, A. Chiralt, C. González-Martínez, Physical properties of edible chitosan films containing bergamot essential oil and their inhibitory action on *Penicillium italicum*, Carbohydr. Polym. 82 (2010) 277–283.

[12] Z.J. Zhang, N. Li, H.Z. Li, X.J. Li, J.M. Cao, G.P. Zhang, D.L. He, Preparation and characterization of biocomposite chitosan film containing *Perilla frutescens* (L.) Britt. essential oil, Ind. Crops Prod. 112 (2018) 660–667.

[13] I. Dib, L. Angenot, A. Mihamou, A. Ziyyat, M. Tits, *Artemisia campestris* L.: Ethnomedicinal, phytochemical and pharmacological review, J. Herb. Med. 7 (2017) 1–10.

[14] A. Akrout, L.A. Gonzalez, H. El Jani, P.C. Madrid, Antioxidant and antitumor activities of *Artemisia campestris* and *Thymelaea hirsuta* from southern Tunisia, Food Chem. Toxicol. 49 (2011) 342–347.

[15] W. Megdiche-Ksouri, N. Trabelsi, K. Mkadmini, S. Bourgou, A. Noumi, M. Snoussi, R. Barbria, O. Tebourbi, K. Ksouri, *Artemisia campestris* phenolic compounds have antioxidant and antimicrobial activity, Ind. Crops Prod. 63 (2015) 104–113.

[16] I. Karabegović, M. Nikolova, D. Veličković, S. Stojičević, V. Veljković, M. Lazić, Comparison of antioxidant and antimicrobial activities of methanolic extracts of the *Artemisia* sp. recovered by different extraction techniques, Chinese J. Chem. Eng. 19 (2011) 504–511.

[17] A. Akrout, H. El Jani, S. Amouri, M. Neffati, Screening of Antiradical and Antibacterial Activities of Essential Oils of *Artemisia campestris* L., *Artemisia* herba *alba Asso*, & *Thymus capitatus Hoff*. Et Link. Growing Wild in the Southern of Tunisia, Recent Res. Sci. Technol. 2 (2010).

[18] M.B. Naili, R.O. Alghazeer, N.A. Saleh, A.Y. Al-Najjar, Evaluation of antibacterial and antioxidant activities of *Artemisia campestris* (Astraceae) and *Ziziphus lotus* (Rhamnacea), Arab. J. Chem. 3 (2010) 79–84.

[19] A. Houicher, E. Kuley, B. Bendeddouche, F. Özogul, Effect of *Mentha spicata* L. and *Artemisia campestris* extracts on the shelf life and quality of vacuum-packed

refrigerated sardine (*Sardina pilchardus*) filletsNo Title, J. Food Prot. 76 (2013) 1719–1725.

[20] I. Chaieb, A. Ben Hamouda, W. Tayeb, K. Zarrad, T. Bouslema, A. Laarif, No TitleThe Tunisian Artemisia Essential Oil for Reducing Contamination of Stored Cereals by *Tribolium castaneum*, Food Technol. Biotechnol. 56 (2018) 247–256.

[21] F. Titouhi, M. Amri, C. Messaoud, S. Hamdi, S. Youssfi, A. Cherif, J. Mediouni-Ben Jemâa, No TitleProtective effects of three Artemisia essential oils against *Callosobruchus maculatus* and *Bruchus rufimanus* (Coleoptera: Chrysomelidae) and the extended side-effects on their natural enemies, J. Stored Prod. Res. 72 (2017) 11–20.

[22] V.G.L. Souza, A.L. Fernando, J.R.A. Pires, P.F. Rodrigues, A.A.S. Lopes, F.M.B. Fernandes, Physical properties of chitosan films incorporated with natural antioxidants, Ind. Crops Prod. 107 (2017) 565–572.

[23] V. Dewanto, W. Xianzhong, K.K. Adom, R.H. Liu, Thermal processing enhances the nutritional value of tomatoes by increasing total antioxidant activity, J. Agric. Food Chem. 50 (2002) 3010–3014.

[24] J. Zhishen, T. Mengcheng, W. Jianming, The determination of flavonoid contents in mulberry and their scavenging effects on superoxide radicals, Food Chem. 64 (1999) 555–559.

[25] I. Dib, M.L. Fauconnier, M. Sindic, F. Belmekki, A. Assaidi, M. Berrabah, H. Mekhfi, M. Aziz, A. Legssyer, M. Bnouham, A. Ziyyat, Chemical composition, vasorelaxant, antioxidant and antiplatelet effects of essential oil of *Artemisia campestris* L. from Oriental Morocco, BMC Complement. Altern. Med. 17 (2017) 82.

[26] R.P. Adams, Identification of essential oil components by gas chromatography, quadrupole mass spectroscopy, 3rd ed., Carol Stream, Ill. : Allured Pub. Corporation, c2001., 2001.

[27] M. Abdollahi, M. Rezaei, G. Farzi, A novel active bionanocomposite film incorporating rosemary essential oil and nanoclay into chitosan, J. Food Eng. 111 (2012) 343–350.

[28] Y. Peng, Y. Wu, Y. Li, Development of tea extracts and chitosan composite films for active packaging materials, Int. J. Biol. Macromol. 59 (2013) 282–289.

[29] A. Silva-Weiss, V. Bifani, M. Ihl, P.J.A. Sobral, M.C. Gómez-Guillén, Structural properties of films and rheology of film-forming solutions based on chitosan and chitosan-starch blend enriched with murta leaf extract, Food Hydrocoll. 31 (2013) 458–

466.

[30] M. Bajić, H. Jalšovec, A. Travan, U. Novak, B. Likozar, Chitosan-based films with incorporated supercritical CO2 hop extract: Structural, physicochemical, and antibacterial properties, Carbohydr. Polym. 219 (2019) 261–268.

[31] J.F. Rubilar, R.M.S. Cruz, H.D. Silva, A.A. Vicente, I. Khmelinskii, M.C. Vieira, Physico-mechanical properties of chitosan films with carvacrol and grape seed extract, J. Food Eng. 115 (2013) 466–474.

[32] ASTM. Standard test methods for tensile properties of thin plastic sheeting, D882-02. In: Annual Book of ASTM Standards. American Society for Testing and Materials, (2002).

[33] Y. Byun, Y.T. Kim, S. Whiteside, Characterization of an antioxidant polylactic acid (PLA) film prepared with α-tocopherol, BHT and polyethylene glycol using film cast extruder, J. Food Eng. 100 (2010) 239–244.

[34] A. Yildirim, A. Mavi, A.A. Kara, Determination of antioxidant and antimicrobial activities of *Rumex crispus* L. extracts, J. Agric. Food Chem. 49 (2001) 4083–4089.

[35] T.C.P. Dinis, V.M.C. Madeira, L.M. Almeida, Action of phenolic derivatives (acetaminophen, salicylate, and 5-aminosalicylate) as inhibitors of membrane lipid peroxidation and as peroxyl radical scavengers, Arch. Biochem. Biophys. 315 (1994) 161–169.

[36] W. Dhifi, S. Bellili, S. Jazi, N. Bahloul, W. Mnif, Essential Oils' Chemical Characterization and Investigation of Some Biological Activities: A Critical Review, Medicines. 3 (2016) 25.

[37] N. Aicha, S. Ines, B.S. Mohamed, B. Ines, K. Soumaya, G. Kamel, N. Aicha, C. Imed, H. Mohamed, C.G. Leila, Chemical composition, mutagenic and antimutagenic activities of essential oils from (tunisian) *Artemisia campestris* and *Artemisia herba-alba*, J. Essent. Oil Res. 20 (2008) 471–477.

[38] Y. Shahbazi, The properties of chitosan and gelatin films incorporated with ethanolic red grape seed extract and *Ziziphora clinopodioides* essential oil as biodegradable materials for active food packaging, Int. J. Biol. Macromol. 99 (2017) 746–753.

[39] I.M. Lipatova, N. V. Losev, L.I. Makarova, J.A. Rodicheva, V.A. Burmistrov, Effect of composition and mechanoactivation on the properties of films based on starch and chitosans with high and low deacetylation, Carbohydr. Polym. 239 (2020) 116245.

[40] C. Wu, J. Tian, S. Li, T. Wu, Y. Hu, S. Chen, T. Sugawara, X. Ye, Structural properties of films and rheology of film-forming solutions of chitosan gallate for food packaging,

Carbohydr. Polym. 146 (2016) 10–19.

[41] M.Á.V. Rodrigues, M.R.V. Bertolo, C.A. Marangon, V. da C.A. Martins, A.M. de G. Plepis, Chitosan and gelatin materials incorporated with phenolic extracts of grape seed and jabuticaba peel: Rheological, physicochemical, antioxidant, antimicrobial and barrier properties, Int. J. Biol. Macromol. 160 (2020) 769–779.

[42] C.A. Lin, T.H. Ku, Shear and elongational flow properties of thermoplastic polyvinyl alcohol melts with different plasticizer contents and degrees of polymerization, J. Mater. Process. Technol. 200 (2008) 331–338.

[43] D.J. McClements, J. Weiss, Lipid Emulsions, in: Bailey's Ind. Oil Fat Prod., Wiley, 2005: pp. 26–34.

[44] Y. Peng, Y. Li, Combined effects of two kinds of essential oils on physical, mechanical and structural properties of chitosan films, Food Hydrocoll. 36 (2014) 287–293.

[45] C.M. Noronha, S.M. De Carvalho, R.C. Lino, J. L.M. Barreto, Characterization of antioxidant methylcellulose film incorporated with α-tocopherol nanocapsules, Food Chem. 159 (2014) 529–535.

[46] S. Salmieri, M. Lacroix, Physicochemical properties of alginate/polycaprolactone-based films containing essential oils, J. Agric. Food Chem. 54 (2006) 10205–10214.

[47] K. Yang, H. Dang, L. Liu, X. Hu, X. Li, Z. Ma, X. Wang, T. Ren, Effect of syringic acid incorporation on the physical, mechanical, structural and antibacterial properties of chitosan film for quail eggs preservation, Int. J. Biol. Macromol. 141 (2019) 876–884.

[48] Y.M. Tan, S.H. Lim, B. T. Tay, M.W. Lee, E.S. Thian, No TitleFunctional chitosan-based grapefruit seed extract composite films for applications in food packaging technology, Mater. Res. Bull. 69 (2015) 142–146.

[49] L. Sun, J. Sun, L. Chen, P. Niu, X. Yang, Y. Guo, Preparation and characterization of chitosan film incorporated with thinned young apple polyphenols as an active packaging material, Carbohydr. Polym. 163 (2017) 81–91.

[50] S.M. Ojagh, M. Rezaei, S.H. Razavi, S.M.H. Hosseini, Development and evaluation of a novel biodegradable film made from chitosan and cinnamon essential oil with low affinity toward water, Food Chem. 122 (2010) 161–166.

[51] X. Zhang, J. Liu, H. Yong, Y. Qin, J. Liu, C. Jin, Development of antioxidant and antimicrobial packaging films based on chitosan and mangosteen (*Garcinia mangostana* L.) rind powder, Int. J. Biol. Macromol. 145 (2020) 1129–1139.

[52] M.H. Hosseini, S.H. Razavi, M.A. Mousavi, Antimicrobial, physical and mechanical

properties of chitosan-based films incorporated with thyme, clove and cinnamon essential oils, J. Food Process. Preserv. 33 (2009) 727–743.

[53] H. Haghighi, S. Biard, F. Bigi, R. De Leo, E. Bedin, F. Pfeifer, H.W. Siesler, F. Licciardello, A. Pulvirenti, Comprehensive characterization of active chitosan-gelatin blend films enriched with different essential oils, Food Hydrocoll. 95 (2019) 33–42.

[54] P. Mayachiew, S. Devahastin, Effects of drying methods and conditions on release characteristics of edible chitosan films enriched with Indian gooseberry extract, Food Chem. 118 (2010) 594–601.

[55] P. Di Pierro, B. Chico, R. Villalonga, L. Mariniello, A.E. Damiao, P. Masi, R. Porta, Chitosan-whey protein edible films produced in the absence or presence of transglutaminase: Analysis of their mechanical and barrier properties, Biomacromolecules. 7 (2006) 744–749.

[56] L. Sánchez-González, A. Chiralt, C. González-Martínez, M. Cháfer, Effect of essential oils on properties of film forming emulsions and films based on hydroxypropylmethylcellulose and chitosan, J. Food Eng. 105 (2011) 246–253.

[57] H. Yong, J. Liu, Y. Qin, R. Bai, X. Zhang, J. Liu, Antioxidant and pH-sensitive films developed by incorporating purple and black rice extracts into chitosan matrix, Int. J. Biol. Macromol. 137 (2019) 307–316.

[58] U. Siripatrawan, B.R. Harte, Physical properties and antioxidant activity of an active film from chitosan incorporated with green tea extract, Food Hydrocoll. 24 (2010) 770–775.

[59] L. Zhang, Z. Liu, X. Han, Y. Sun, X. Wang, Effect of ethanol content on rheology of film-forming solutions and properties of zein/chitosan film, Int. J. Biol. Macromol. 134 (2019) 807–814.

[60] U. Siripatrawan, W. Vitchayakitti, Improving functional properties of chitosan films as active food packaging by incorporating with propolis, Food Hydrocoll. 61 (2016) 695–702.

[61] Y. Peng, Q. Wang, J. Shi, Y. Chen, X. Zhang, Optimization and release evaluation for tea polyphenols and chitosan composite films with regulation of glycerol and tween, Food Sci. Technol. 40 (2020) 162–170.

[62] C. Qiao, X. Ma, J. Zhang, J. Yao, Effect of hydration on water state, glass transition dynamics and crystalline structure in chitosan films, Carbohydr. Polym. 206 (2019) 602–608.

[63] L. Ren, X. Yan, J. Zhou, J. Tong, X. Su, Influence of chitosan concentration on

mechanical and barrier properties of corn starch/chitosan films, Int. J. Biol. Macromol. 105 (2017) 1636–1643.

[64] X. Zhang, H. Lian, J. Shi, W. Meng, Y. Peng, Plant extracts such as pine nut shell, peanut shell and jujube leaf improved the antioxidant ability and gas permeability of chitosan films, Int. J. Biol. Macromol. 148 (2020) 1242–1250.

[65] C. Valenzuela, L. Abugoch, C. Tapia, Quinoa protein-chitosan-sunflower oil edible film: Mechanical, barrier and structural properties, LWT - Food Sci. Technol. 50 (2013) 531–537.

[66] S. Mali, M.V.E. Grossmann, M.A. Garcia, M.N. Martino, N.E. Zaritzky, Microstructural characterization of yam starch films, Carbohydr. Polym. 50 (2002) 379–386.

[67] L. Sánchez-González, C. González-Martínez, A. Chiralt, M. Cháfer, Physical and antimicrobial properties of chitosan-tea tree essential oil composite films, J. Food Eng. 98 (2010) 443–452.

[68] A. Perdones, L. Sánchez-González, A. Chiralt, M. Vargas, Effect of chitosan-lemon essential oil coatings on storage-keeping quality of strawberry, Postharvest Biol. Technol. 70 (2012) 32–41.

[69] J. Sun, H. Jiang, H. Wu, C. Tong, J. Pang, C. Wu, Multifunctional bionanocomposite films based on konjac glucomannan/chitosan with nano-ZnO and mulberry anthocyanin extract for active food packaging, Food Hydrocoll. 107 (2020) 105942.

[70] E. Jahed, M.A. Khaledabad, H. Almasi, R. Hasanzadeh, Physicochemical properties of Carum copticum essential oil loaded chitosan films containing organic nanoreinforcements, Carbohydr. Polym. 164 (2017) 325–338.

[71] A. L, A. Chiralt, Chiralt, Essential oils as additives in biodegradable films and coatings for active food packaging, Trends Food Sci. Technol. 48 (2016) 51–62.

[72] B. He, W. Wang, Y. Song, Y. Ou, J. Zhu, Structural and physical properties of carboxymethyl cellulose/gelatin films functionalized with antioxidant of bamboo leaves, Int. J. Biol. Macromol. 164 (2020) 1649–1656.

[73] A. Djeridane, M. Yousfi, B. Nadjemi, N. Vidal, J.F. Lesgards, P. Stocker, Screening of some Algerian medicinal plants for the phenolic compounds and their antioxidant activity, Eur. Food Res. Technol. 224 (2007) 801–809.

[74] J. Graßmann, Terpenoids as Plant Antioxidants, in: G. Litwack (Ed.), Vitam. Horm., Academic Press, 2005: pp. 505–535.

Table 1

Chemical composition of *Artemisia campestris* essential oil analyzed by GC-MS.

Peak No.	RI	Compound	Composition (%)
1	926	α-Thujene	0.4
2	932	α-Pinene	8.73
3	977	β-Pinene	25.67
4	992	β-Myrcene	7.54
5	1016	α-Terpinene	1.26
6	1026	p-cymene	8.26
7	1030	Limonene	15.39
8	1040	Cis-Ocimene	4.98
9	1050	TRANS-β.-OCIMENE	4.57
10	1060	γ-Terpinene	10.48
11	1089	α-terpinolene	0.73
12	1180	l-4-Terpineol	0.95
13	1378	α-Copaene	0.49
14	1385	Geranyl acetate	0.97
15	1484	D-germacrene	2.34
16	1518	γ-Cadinene	0.27
17	1527	δ-Cadinene	1.16
18	1568	Trans nerolidol	0.51
19	1584	Spathulenol	0.83
20	1611	Geranyl isovalerate	1.58
21	1658	β-Eudesmol	1.83
		Monoterpene hydrocarbons	88.01
		Oxygenated monoterpenes	3.5
		Sesquiterpene hydrocarbons	4.26
		Oxygenated sesquiterpenes	3.17
		Total identified	98.94

RI: Retention indices

Identification Method: Comparison of RIs and mass spectra with Data from MS library and the literature.

Table 2

Extraction yield, total phenolic and flavonoid contents in *Artemisia campestris* hydroalcoholic extract (ACHE) and aqueous extract (ACAE).

Extract	Yield extraction (%, w/dw)	Total polyphenols (mg GAE/g extract)	Flavonoids (mg QE/g extract)
ACHE	16.81 [a] ± 0.51	269.98 [a] ± 4.18	195.12 [a] ± 3.32
ACAE	13.17 [b] ± 0.51	101.19 [b] ± 3.47	79.80 [b] ± 3.83

Values are presented as mean ± standard deviation. Different letters in the same column indicate significant differences ($p < 0.05$).

Table 3

Power law parameters of different film-forming solutions.

Film	n	k (Pa·s)^n	η_{ap} (Pa·s) (at 0.1 s^{-1})	η_{ap} (Pa·s) (at 100 s^{-1})
CH	0.824 [a] ± 0.008	0.676 [a] ± 0.021	0.882 [a] ± 0.019	0.342 [a] ± 0.011
CH-ACHE	0.915 [b] ± 0.022	0.340 [b] ± 0.020	0.4 [b] ± 0.028	0.240 [b] ± 0.009
CH-ACAE	0.875 [a] ± 0.039	0.021 [c] ± 0.003	0.029 [c] ± 0.004	0.012 [c] ± 0.000
CH-ACEO	0.918 [b] ± 0.002	0.515 [d] ± 0.001	0.601 [d] ± 0.006	0.354 [a] ± 0.002

n: flow behavior index; k: consistency index; $\eta_{ap:}$ apparent viscosity.
Values are presented as mean ± standard deviation. Different letters in the same column indicate significant differences ($p < 0.05$).

Table 4

Physical and mechanical properties of CH, CH-ACHE, CH-ACAE and CH-ACAE films.

Film	Thickness (mm)	MC (%)	WS (%)	SW (%)	TS (MPa)	EAB (%)
CH	0.171 [a] ± 0.07	36.09 [a] ± 0.59	18.30 [a] ± 0.55	88.28 [a] ± 2.30	2.43 [a] ± 0.40	89.71 [a] ± 2.46
CH-ACHE	0.190 [b] ± 0.007	26.34 [b] ± 0.16	15.89 [b] ± 0.97	81.45 [b] ± 1.39	1.69 [b] ± 0.15	89.72 [a] ± 3.18
CH-ACAE	0.134 [c] ± 0.011	27.46 [b] ± 0.73	30.92 [c] ± 1.05	53.85 [c] ± 1.03	0.89 [c] ± 0.18	13.34 [b] ± 1.75
CH-ACEO	0.21 [d] ± 0.013	30.49 [c] ± 0.87	12.80 [d] ± 1.70	90.38 [a] ± 1.27	2.19 [a] ± 0.20	65.20 [c] ± 4.64

MC: moisture content; WS: water solubility; SW: swelling index; TS: tensile strength; EAB: elongation at break.
Values are presented as mean ± standard deviation. Different letters in the same column indicate significant differences ($p < 0.05$).

Table 5

Optical properties of CH, CH-ACHE, CH-ACAE and CH-ACAE films.

Film	L*	a*	b*	ΔE*	C*	Opacity ($A.mm^{-1}$)
CH	96.995 [a] ± 0.085	-0.94 [a] ± 0.030	6.285 [a] ± 0.225	nd	6,355 [a] ± 0.227	0.47 [a] ± 0.02
CH-ACHE	74.323 [b] ± 0.62	3.367 [b] ± 0.335	75.48 [b] ± 0.385	72.946 [a] ± 0.496	75.557 [b] ± 0.323	6.37 [b] ± 0.3
CH-ACAE	71.16 [c] ± 0.760	15.455 [c] ± 0.752	77.985 [c] ± 0.308	77.957 [b] ± 0.630	79.502 [c] ± 0.443	6.67 [b] ± 0.15
CH-ACEO	97.63 [a] ± 0.22	-1.515 [a] ± 0.135	13.505 [d] ± 0.085	7.275 [c] ± 0.362	13.590 [d] ± 0.377	1.63 [c] ± 0.02

nd: not determined

Values are presented as mean ± standard deviation. Different letters in the same column indicate significant differences ($p < 0.05$)

Table 6

Weight loss (ΔW), transformation temperature (T and Tmax) and % of residue obtained by the thermogravimetric analysis of CH, CH-ACHE, CH-ACAE and CH-ACAE films.

Film	Phase I			Phase II			Phase III			Phase IV			Residue (%)
	ΔW (%)	T (°C)	Tmax (°C)	ΔW (%)	T (°C)	Tmax (°C)	ΔW (%)	Td (°C)	Tmax (°C)	ΔW (%)	T (°C)	Tmax (°C)	
CH	3.78 [a]	70-128	104 [a]	17.55 [a]	136-225	180 [a]	35.18 [a]	235-400	285 [a]	nd	nd	nd	28.16 [a]
CH-ACHE	4.86 [b]	78-128	102 [b]	16.15 [b]	141-224	182 [b]	38.10 [b]	229-396	281 [b]	7.3 [a]	414-470	438 [a]	31.43 [b]
CH-ACAE	5.37 [c]	69-125	101 [b]	15.37 [c]	134-219	183 [bc]	37.52 [c]	228-404	287 [a]	nd	nd	nd	32.96 [b]
CH-ACEO	2.50 [d]	70-99	87 [c]	19.43 [d]	109-227	179 [c]	32.58 [d]	235-238	280 [b]	16.19 [b]	344-395	365 [b]	22.46 [c]

nd: not determined.

T: Degradation temperature range, Tmax: Maximum temperature.

Means with different superscripts (a-d) within the same column indicate significant differences ($p < 0.05$).

Figure captions

Fig.1. Effect of *Artemisia campestris* extracts on the apparent viscosity of chitosan film-forming solutions.

Fig.2. UV-Vis barrier property of CH, CH-ACHE, CH-ACAE and CH-ACAE films.

Fig.3. FTIR spectra of CH, CH-ACHE, CH-ACAE and CH-ACAE films.

Fig.4. X-ray diffraction patterns of different films: CH, CH-ACHE, CH-ACAE and CH-ACAE.

Fig.5. Scanning electron micrographs of chitosan composite films with *Artemisia campestris* extracts. CH film surface (A) and cross section (a), CH-ACHE film surface (B) and cross section (b), CH-ACAE film surface (C) and cross section (c) and CH-ACEO film surface (D) and cross section. Magnification was ×3000 for A, B, C and D; ×400 for a and c; ×300 for b and ×250 for d. Scale bars are given in each case.

Fig.6. TG curves (A) and DTG thermograms (B) of CH, CH-ACHE, CH-ACAE and CH-ACAE films.

Fig.7. Antioxidant properties of CH, CH-ACHE, CH-ACAE and CH-ACAE films.

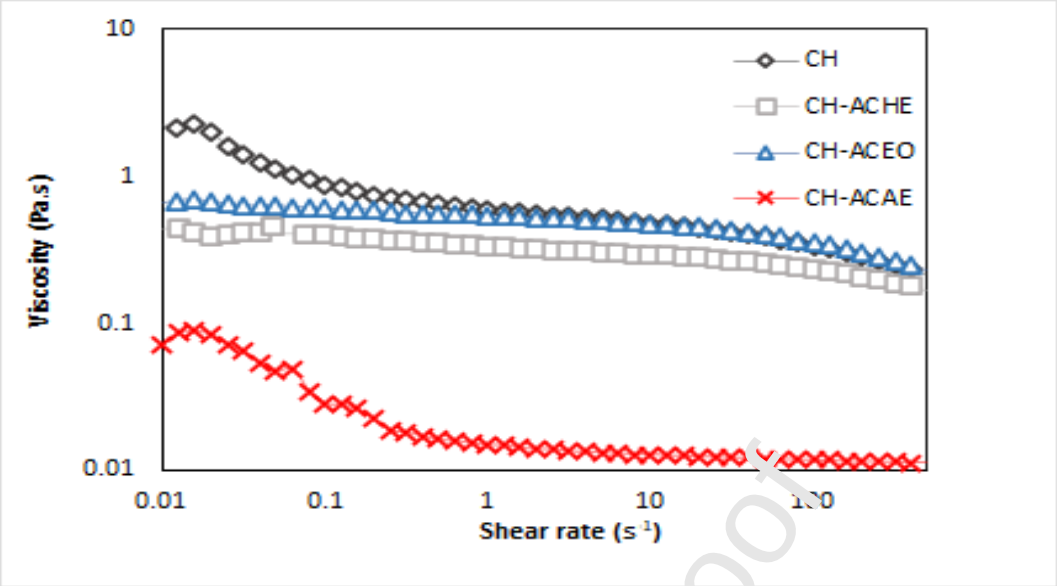

Figure 1

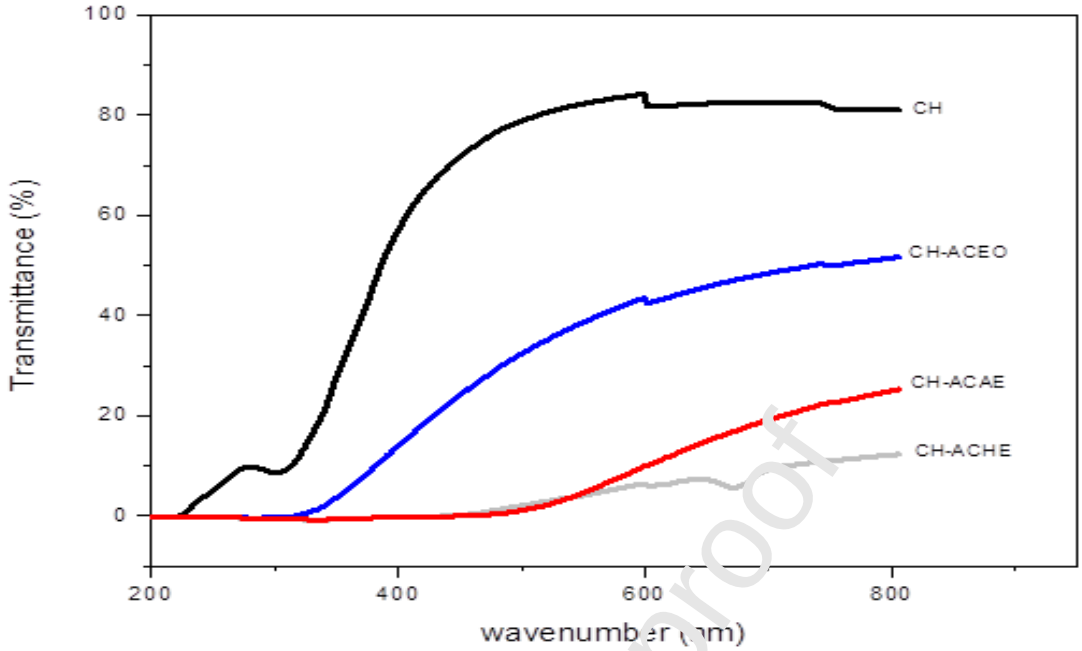

Figure 2

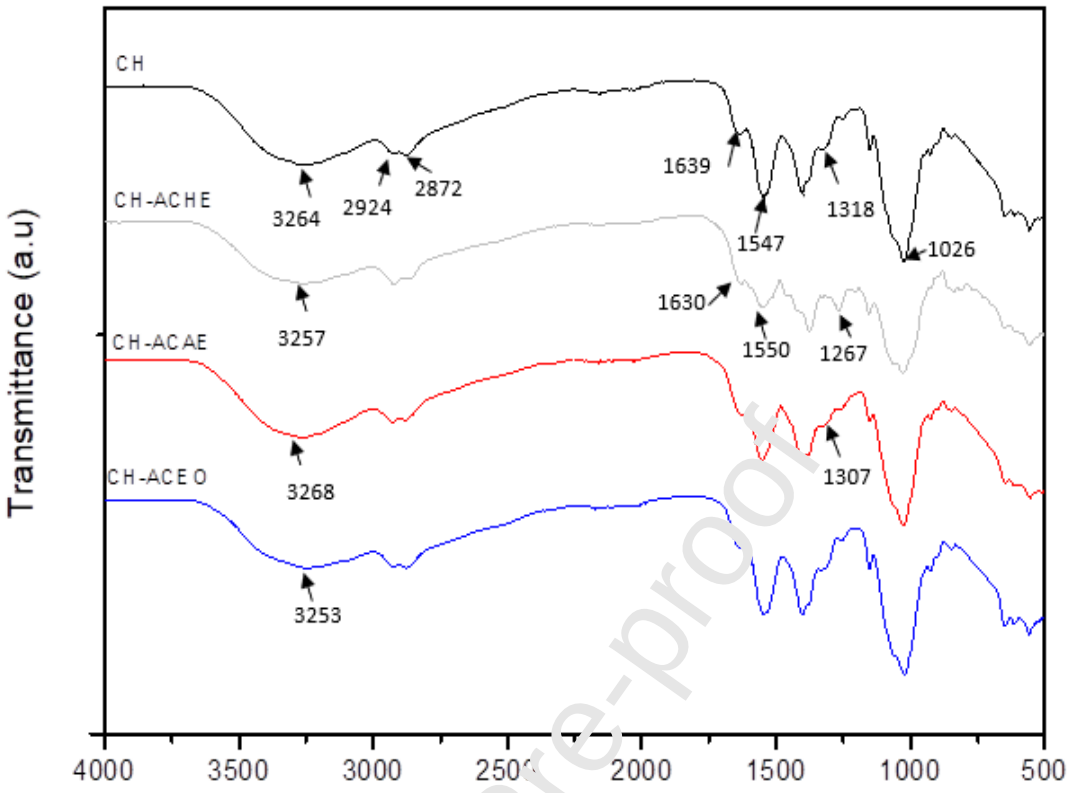

Figure 3

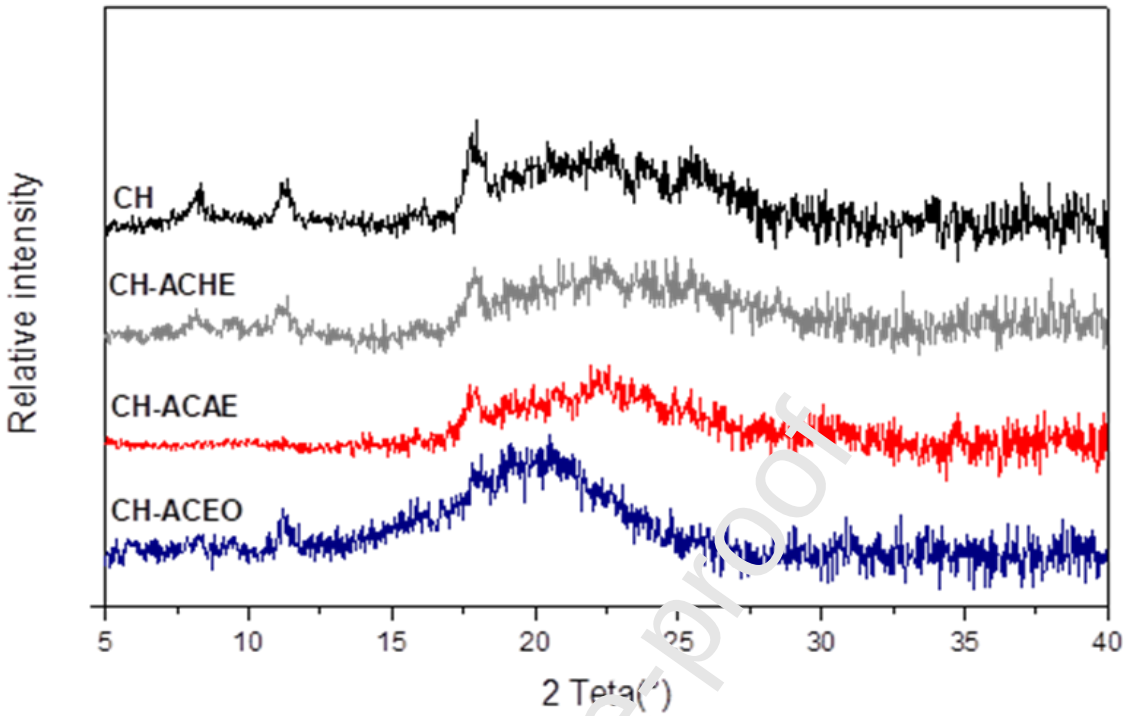

Figure 4

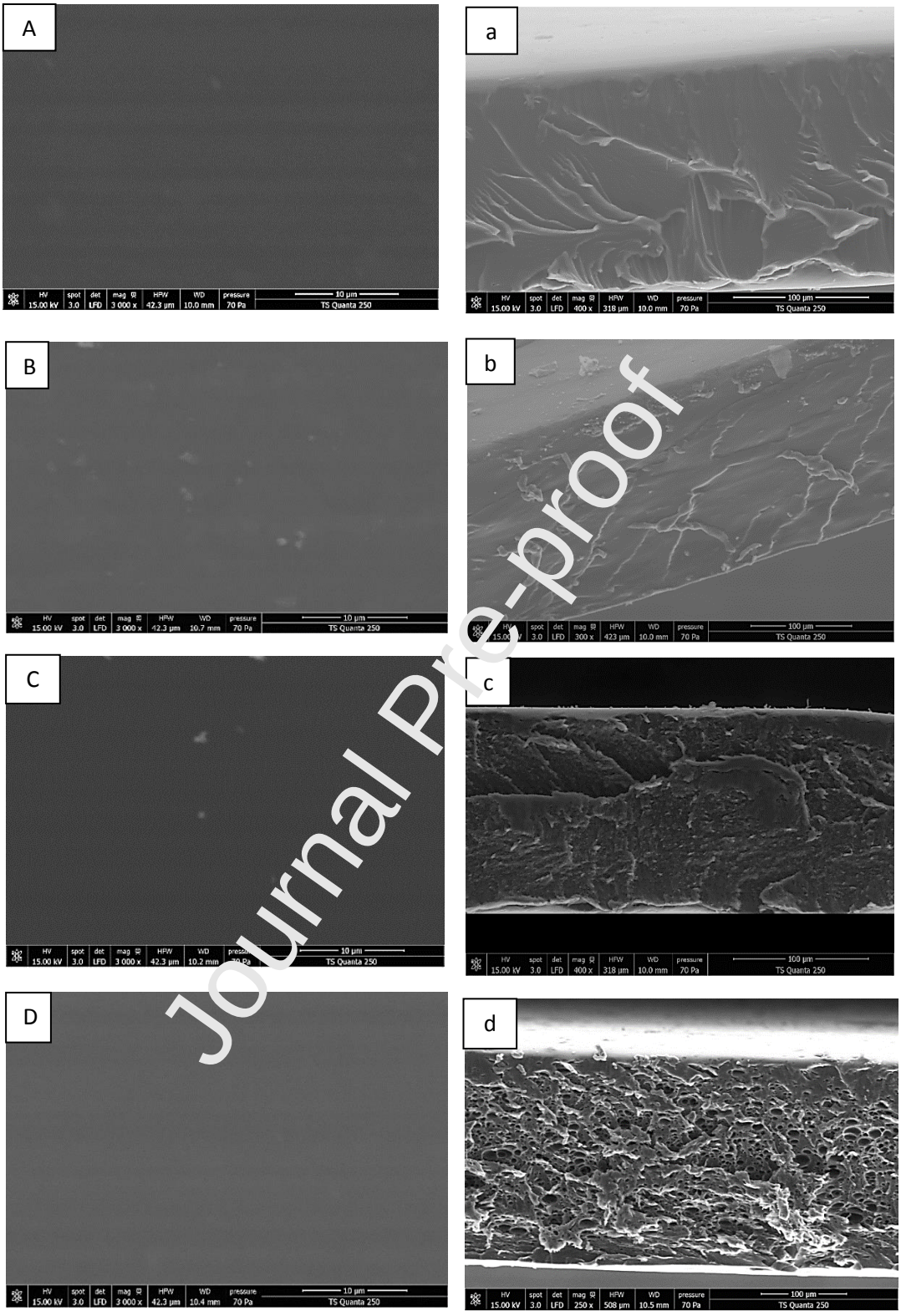

Figure 5

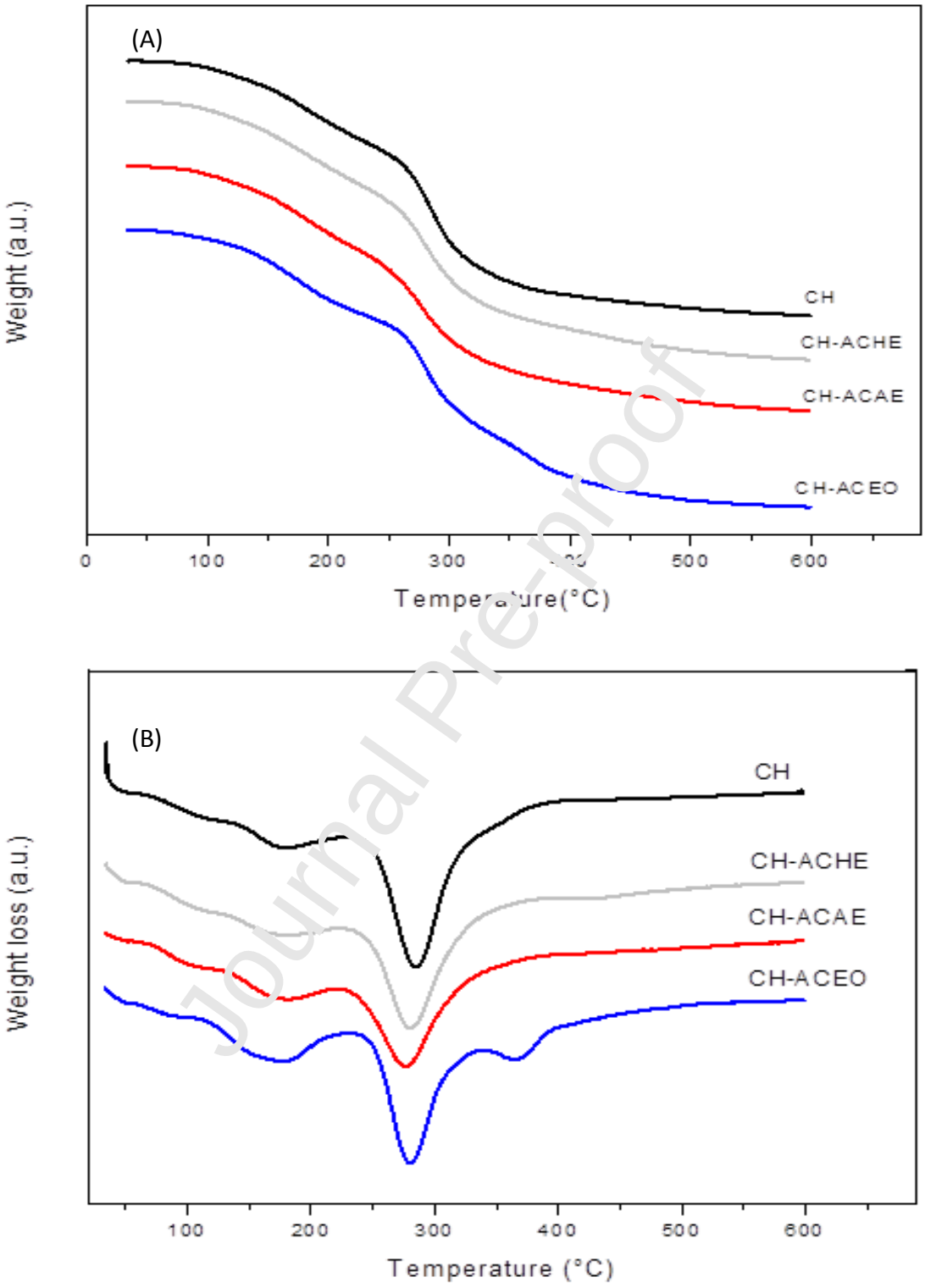

Figure 6

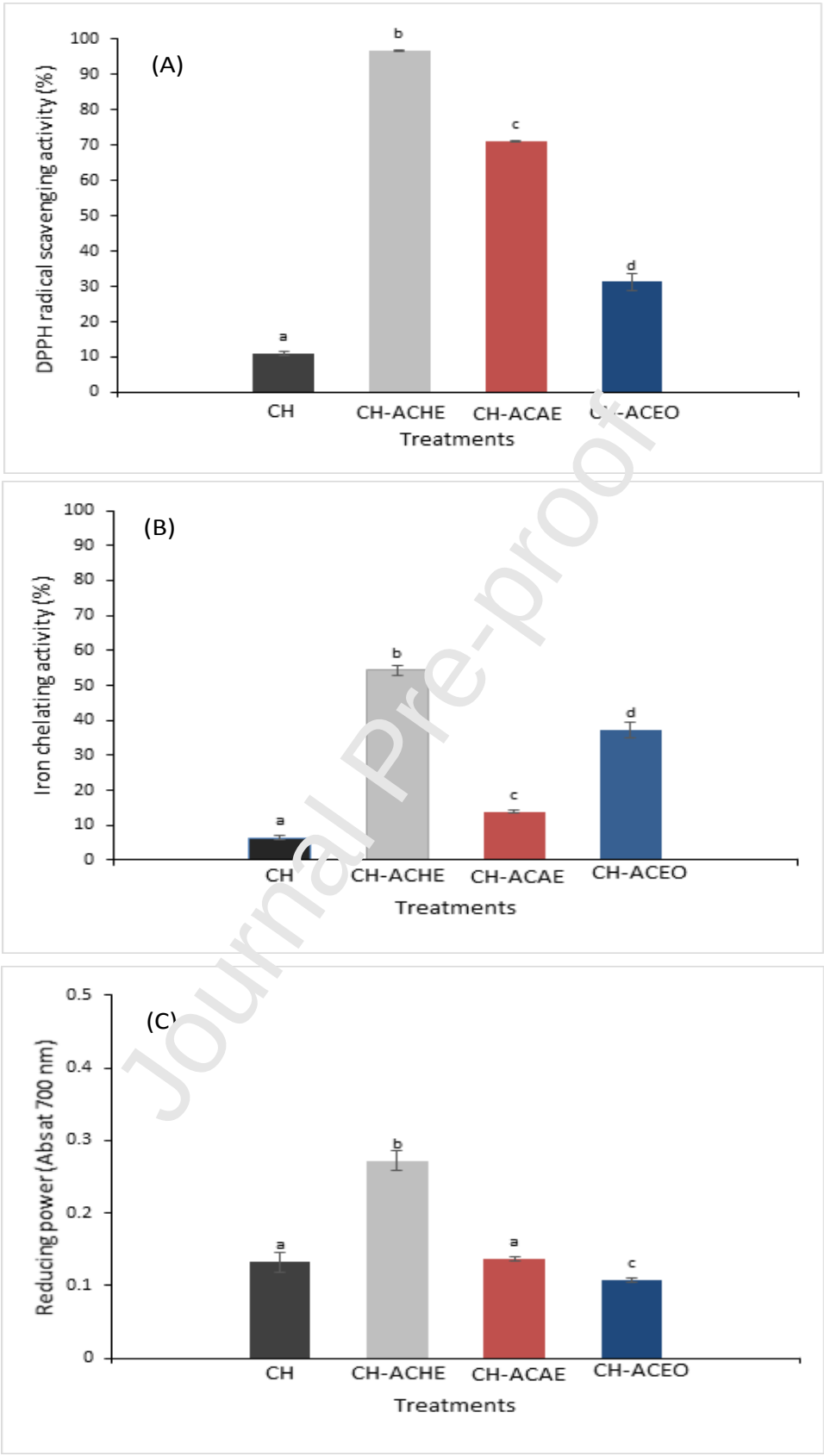
(A)
DPPH radical scavenging activity (%)
100
90
80
70
60
50
40
30
20
10
0
a
b
c
d
CH
CH-ACHE
CH-ACAE
CH-ACEO
Treatments
(B)
Iron chelating activity (%)
100
90
80
70
60
50
40
30
20
10
0
a
b
c
d
CH
CH-ACHE
CH-ACAE
CH-ACEO
Treatments
(C)
Reducing power (Abs at 700 nm)
0.5
0.4
0.3
0.2
0.1
0
a
b
a
c
CH
CH-ACHE
CH-ACAE
CH-ACEO
Treatments

Figure 7

CRediT author statement

All persons who meet authorship criteria are listed as authors, and all authors certify that they have participated sufficiently in the work to take public responsibility for the content, including participation in the concept, design, analysis, writing, or revision of the manuscript.

Authorship contributions:

Salma Moalla: Conceptualization, Methodology, Investigation, Writing - Original draft, Imène Ammar: Methodology, Writing - Review & Editing, Marie-Laure Fauconnier: Investigation, Resources, Sabine Danthine: Investigation, Resources, Christophe Blecker: Supervision, Conceptualization, Resources, Souhail Besbes: Supervision, Hamadi Attia: Conceptualization, Supervision, Writing - review & editing Resources.

Highlights

1. Development of chitosan films enriched with *Artemisia campestris* antioxidant compounds.
2. *Artemisia campestris* ingredients affected the physical-mechanical and structural properties of the films.
3. Enriched films displayed higher UV light barrier and antioxidant potential.
4. Enriched films can serve as active packaging materials.